Proceedings World Geothermal Congress 2020+1
Reykjavik, Iceland, April - October 2021

Utilization of Waste Brine To Enhance an Existing Production Through Hydrothermal Turbine And Double Flash Cycle (Back Pressure) in Lahendong Geothermal Field, Indonesia

Adhiguna Satya Nugraha[1], Priatna Budiman[1], Tumpal Parulian Nainggolan[1], Ahmad Yani[1], Salvius Patangke[1], Páll Valdirmarsson[2]

[1]PT Pertamina Geothermal Energy, Area Lahendong, Jalan Raya Tomohon No. 420, Tomohon 95431, Sulawesi Utara, Indonesia

[2]Reykjavík University, School of Science and Engineering, Iceland

adhiguna.nugraha@pertamina.com

Keywords: Indonesia, PT Pertamina Geothermal Energy, Lahendong, Tompaso, Geothermal, Double Flash, Hydrothermal, Expander Turbine.

ABSTRACT

Currently in Indonesia, most of the geothermal sources have two phase dominated fields and use brine from production wells or separators just to maintain the reservoir through reinjection wells. In unit V and VI Lahendong field, steam fractions measured about 20% each and the rest is waste product (hot brine). Then the steam flows into the turbine to generate electricity 2 x 20 MW.

This paper will focus on how to enhance production from waste brine through designing a secondary turbine with a hydrothermal turbine and double flash cycle (back pressure) before waste product is sent into the reinjection wells.

The process design and simulation will use pipe size 6" schedule 40 as brine supply to the facility, either to the flash separator or hydrothermal turbine to avoid disturbance of operation. From the optimization, the double flash cycle (back pressure turbine) resulted in a power output of 2447.56 kW with a differential pressure between the flasher valve and separator of 3.8 bara.

The boiling liquid was applied into the two phase expander (turbo expander type). The turbo expander was able to generate electricity at about 282.23 kW with an outlet pressure of 5.924 bara, while the atmospheric pressure was around 0.924 bara. This type has way to expand the energy by removing the vapor energy from the system. The aim of pressure setting in this research is to reach a silica saturation index (SSI) less than 1 after some processes.

1. INTRODUCTION

PT Pertamina Geothermal Energy has five working areas. One of them is located in North Sulawesi of Indonesia, Lahendong area as shown in Figure 1. Total production capacity of the Lahendong field in 2019 is 120 MW, which is supplied by 6 units from the power plant. Unit I to IV have resources from the Lahendong area and Unit V to VI have resources from the Tompaso area with a distance of about 18 km.

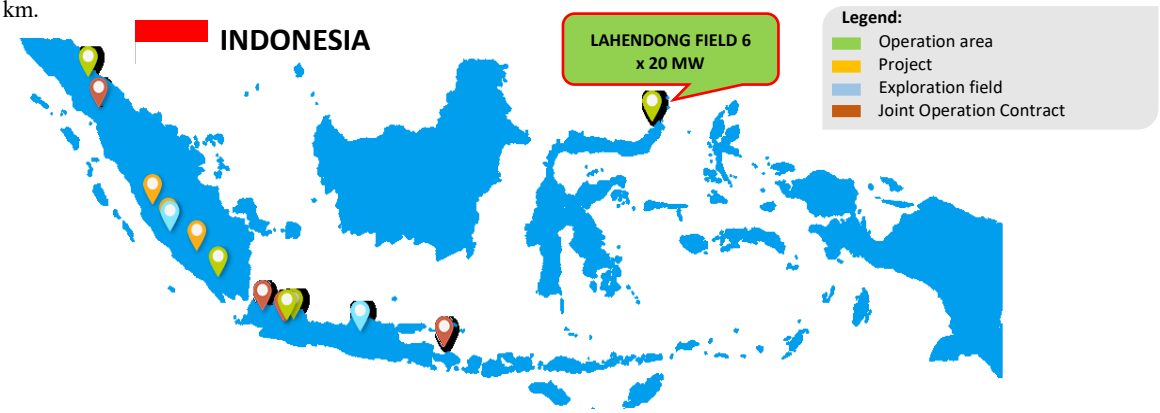

Figure 1: Location of Lahendong geothermal field 6 x 20 MW, North Sulawesi, Indonesia (PT PGE, 2019)

1.1 General backgrounds

Tompaso's field in the Lahendong area has 2 x 20 MW with total project schemes, this means PT Pertamina Geothermal Energy operates the steam field and power plant, exclude electricity distribution due to operation by the National Electricity Company. This field is two phase dominated in geothermal system classification and consists of one cluster of production wells in addition to two clusters of reinjection wells. There are:

1. Production wells
   - Cluster 27: LHD-27, LHD-31, LHD-34, LHD-42, LHD-43.

   The three production wells from LHD-27, LHD-31, and LHD-34 supply the steam to generating power plant unit V, and the other two deliver the steam into power plant unit VI.

2. Reinjection wells
   - Cluster R-1: LHD-41, LHD-46;
   - Cluster R-2: LHD-40 & LHD-44.

1.2 Tracer flow test result in unit V and VI wells

The steam and water flow have been measured during operation with tracer flow test method. The test was performed two to three times between 2016 and 2017 as shown in Table 1. The setting of wellhead pressure was previously based on well testing after drilling was completed.

Table 1: Tracer flow test result of unit V and VI wells (PT PGE, 2017)

Well	Date	WHP (barg)	Throttle open (%)	Steam	Water	Total	Enthalpy (kJ/kg)	Dryness (%)
				ton/hr				
Unit V wells								
LHD-27	3 Oct 2016	16.9	25	45.72	192.96	238.68	1118.2	19.18
	21 Apr 2017	16.7	24	26.9	190.13	217.03	1114.7	12.39
	23 Oct 2017	15.89	24	39.85	176.8	216.65	1123.16	18.39
LHD-31	4 Oct 2016	15.5	28	45.72	344.52	390.24	965.8	11.72
	21 Apr 2017	14.57	28	35.4	223.43	258.83	1116.8	13.68
	23 Oct 2017	13.91	28	40.82	248.95	289.77	1037.78	14.09
LHD-34	3 Oct 2016	31.4	23	57.6	241.92	299.52	1118.7	19.2
	21 Apr 2017	29.88	30	94.8	299.61	394.41	1442.5	24.04
	23 Oct 2017	29.24	36	69.82	252.45	322.27	1191.02	21.67

2. STUDY DESCRIPTION

The pressurized water and hot water inside the pipe from the separator outlet have potential to utilize, by means of using working pressure to then convert into the head value (elevation). With this approach, the working pressure of the separator is directly proportional to the head value to be obtained. In outline, the pressurized water and its flow rate before entering the reinjection wells will be planned to branch out toward to new location, where the turbine will be placed. The mixture of water and vapor discharge from the hydrothermal turbine will go to a thermal pond mixed with steam condensate and emergency dump valve discharge, then pumped to the reinjection wells to maintain the reservoir.

The process flow diagram of unit V and VI in Figure 2 below describes how the two phase fluids from five production wells move through the power plant station. The fluids will pass through a separation process in the separator vessel, where the efficiency value of separator greatly affects the amount of vapor and water separated.

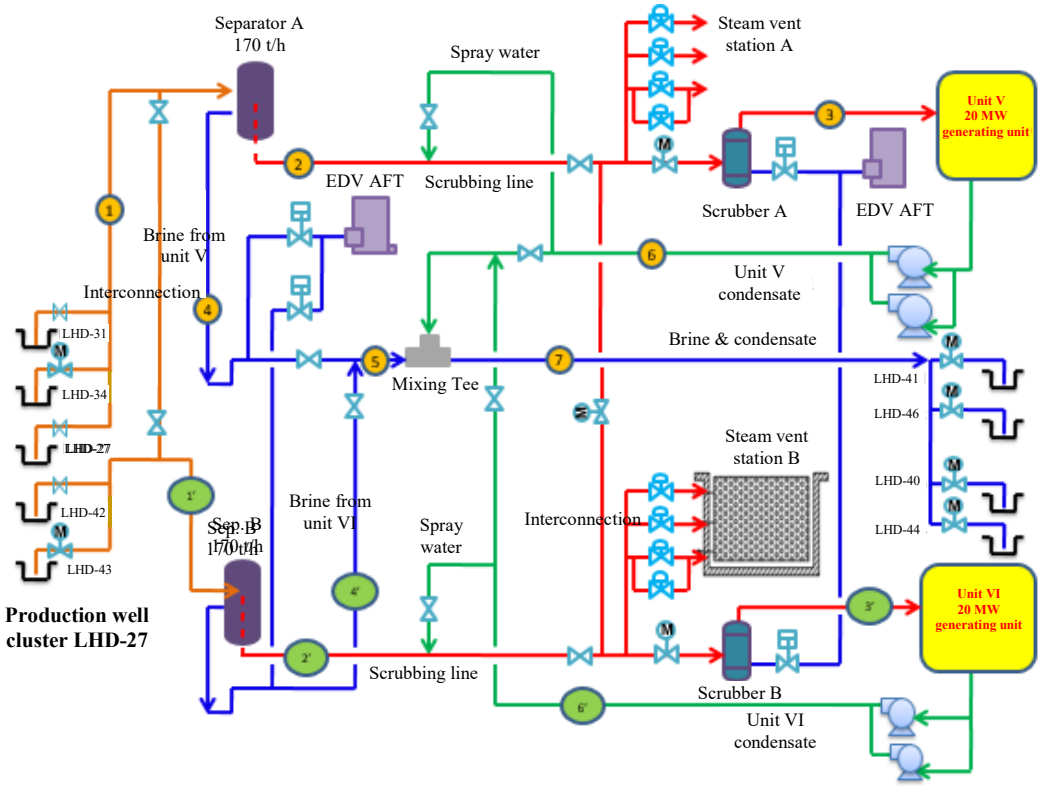

Figure 2: Process flow diagram of Unit V and VI in Lahendong geothermal field, 2 x 20 MW

The operation and production parameters of unit V and VI at design condition as shown on the Table 2 below.

Table 2: Operation and production parameters of Lahendong unit V and VI at design condition

No.	Description	Uom	Stream number					
			1	1"	2	2"	3	3"
1.	Pressure	bara	8.9	8.87	8.6	8.57	8	8
2.	Temperature	°C	174.9	174.7	173.4	173.3	170.2	170.2
3.	Enthalpy	kJ/kg	1118.9	1118.4	2767.1	2767.0	2768.12	2768.12
4.	Mass flow rate	ton/hr	716.1	716.1	135.2	135.2	133.11	133.11
		kg/s	180.45	180.45	34.07	34.07	33.54	33.54
No.	**Description**	**Uom**	**Stream number**					
			4	**4"**	**5**	**6**	**6"**	**7**
1.	Pressure	bara	8.6	8.6	8.8	13	13	12.9
2.	Temperature	°C	174.4	173.3	173.3	38.5	38.5	164.3
3.	Enthalpy	kJ/kg	734.2	733.6	738.2	162.5	162.5	694.8
4.	Mass flow rate	ton/hr	580.9	580.8	1161.7	39.5	39.5	1240.7
		kg/s	146.38	146.36	292.74	9.95	9.95	312.65

From process design data, the total flow of two phase fluids from wells to separator A/B is about 180.45 kg/s each, then pressure setting on the separator is 8.9 bara and 8.87 bara. The steam heads towards the turbine with an inlet pressure of 8 bara and a steam flow of about 34.07 kg/s to the scrubber station. The separated water stream has a flowrate around 146.38 kg/s from separator A and 146.36 kg/s from separator B with a working pressure of 8.6 bara. In addition, the existing production facility will have some modification in the main line of brine pipe as described in Figure 3 to obtain some new parameters for design.

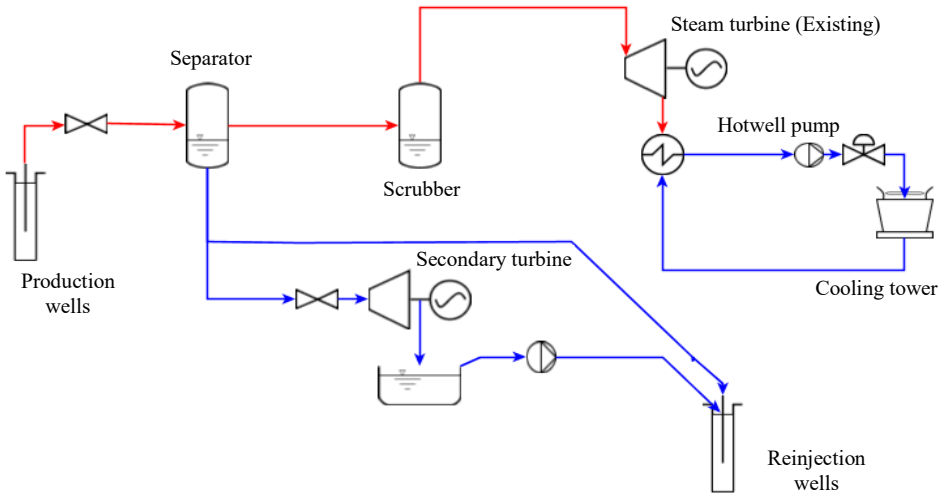

Figure 3: Schematic diagram of hydrothermal turbine

3. THEORETICAL BACKGROUND

3.1 Pipe design

The cross sectional area inside of pipe can be defined:

$$A = \frac{1}{4} \cdot \pi \cdot D_{in}^2 \tag{1}$$

Velocity of fluids:

$$V = \frac{m}{A \cdot \rho} \tag{2}$$

The pipe thickness (required and minimum) according to power piping standard:

$$t_r = \frac{P \cdot D}{2 \cdot (S \cdot E + P \cdot Y)} \tag{3}$$

$$t_m = t_r + CA \tag{4}$$

3.2 Pressure drop analysis

The Reynolds number should be calculated using equation:

$$Re = \frac{\rho \cdot V \cdot D_{in}}{\mu} \tag{5}$$

Based on the Reynolds number, friction factor should be calculated from equation 6 below, the Darcy friction factor and equation 7, called the Swanee-Jain equation, used to solve the Darcy-Weisbach friction factor for a full-flowing circular pipe as approximation of the implicit Colebrook-White equation.

$$Re \leq 2100, \qquad \mathrm{f} = \frac{64}{Re} \tag{6}$$

$$Re > 2100, \qquad \mathrm{f} = \frac{0.25}{\left(log_{10} \left[\frac{\epsilon}{\frac{D_{in}}{3.7}} + \frac{5.74}{Re^{0.9}} \right] \right)^2} \tag{7}$$

The friction head can be calculated by:

$$H_f = \frac{f \cdot V^2 \cdot Le}{2 \cdot g \cdot D_{in}} \tag{8}$$

Then the pressure drop due to friction along the pipeline and the elevation difference can be explained by:

$$\Delta P_f = \rho \cdot g \cdot H_f \tag{9}$$

$$\Delta P_H = \rho \cdot g \cdot (Z_s - Z_e) \tag{10}$$

Furthermore, the total pressure drop along the pipeline systems can be summarized:

$$\Delta P_t = \Delta P_f + \Delta P_H \tag{11}$$

3.3 Heat loss analysis

To calculate the overall heat transfer on a cylinder plane inside and outside of pipe, it is conducted by dividing the temperature difference by the total thermal resistance between two surfaces (Ohm law):

$$q = \frac{\Delta T}{R} \tag{12}$$

$$q = \frac{\Delta T}{R_{conv,1} + R_1 + R_2 + R_3 + R_{conv,2}}$$

$$R = \frac{1}{hi \cdot 2 \cdot \pi \cdot r_1 \cdot L} + \frac{\ln r_2/r_1}{2 \cdot \pi \cdot k_1 \cdot L} + \frac{\ln r_3/r_2}{2 \cdot \pi \cdot k_2 \cdot L} + \frac{\ln r_4/r_3}{2 \cdot \pi \cdot k_3 \cdot L} + \frac{1}{ho \cdot 2 \cdot \pi \cdot r_4 \cdot L} \tag{13}$$

$$\frac{q}{L} = \frac{2 \cdot \pi \cdot (T_{in} - T_{out})}{\frac{1}{hi \cdot r_1} + \frac{\ln r_2/r_1}{k_1} + \frac{\ln r_3/r_2}{k_2} + \frac{\ln r_4/r_3}{k_3} + \frac{1}{ho \cdot r_4}} \tag{14}$$

$$\Delta T = \frac{q}{m \cdot Cp_l} \tag{15}$$

3.4 Two phase expanders (Hydrothermal turbine)

In order to utilize hot water as resource to generate electricity and flash saturated liquid when it flows into turbine, we should find the appropriate turbine with the two-phase working fluids. The two phase expanders can operate with mixture fluids as well that will appear at the end of the expansion process, meaning it is able to handle the presence of a liquid phase during expansion (wet fluids), where the fluid is in two-phase state at the expander outlet.

Figure 4: Turbo expander (Kimmel and Cathery, 2010)

Generally, the turbo or turbine expander (dynamic type) is suitable for power output greater than 50 kW and this type allows pressure reduction into the vapor phase, but takes advantage of the buoyant and convective forces of released vapor by routing the fluid in an upward direction such that the flow is aided by these forces (Kimmel, 2010).

The common technology of turbo expander has been proved in LNG plant, when the expansion process generates some vapor and ensure it remains in the liquid phase at the outlet expanders with a back pressure around 5 bar above the liquid bubble point (Kimmel, 2010).

Based on experiences that had been taken previously by a professional in industry (two-phase region of LNG) and has proven for several years, then this paper would discuss turbo expander in Figure 4 as driver to generate electricity and expand the steam flash from saturated or boiling liquid. Two phase expander design concepts essentially follow existing single-phase and expander technology, which is the energy from pressurized hot water converted to electrical energy, then into kinetic energy, then into mechanical shaft power and finally to electrical energy through the use of an electrical power generator.

The two phase expanders do not take into account vaporization during the phase changes in the process and the efficiency is applicable to expanders (turbine) driven by boiling liquid, when boiling occurs inside the turbine (Finley, 2006).

To calculate the turbo expander efficiency will be defined by using the equation:

$$\eta_{one\_phase} = \frac{W_{generator\_out}}{\dot{m} \cdot (h_1 - h_2)} \tag{16}$$

When the vaporization occurred in the process, a substance exits as part liquid and part vapor, it should find the quality as the ratio of the vapor mass to the total mass (mixture):

$$x = \frac{m_{vapor}}{m_{total}} \tag{17}$$

$$m_{total} = m_{liquid} + m_{vapor} \tag{18}$$

The enthalpy of a two phase fluids can be defined as:

$$h_{av} = h_f + x \cdot h_{fg} \tag{19}$$

During the vaporization process, the enthalpy of it applies no work to the system, thus the vapor energy will be removed in term from the efficiency calculation. The energy used in the vaporization process can be found as follow:

$$h_{vap} \cdot (x_{out} - x_{in}) \tag{20}$$

Furthermore, the useful change in enthalpy can be applied to the expander shaft as work is:

$$\Delta h = h_{av\_in} - [h_{av\_out} - h_{vap} \cdot (x_{out} - x_{in})] \tag{21}$$

Since h_{av_in} and h_{av_out} are the total enthalpies of the saturated mixture, this total useful enthalpy change is equal to the work output in an ideal (100% efficient two phase expander). Therefore, the maximum possible work output from an ideal two phase expander is (could be converted to electricity):

$$W_{max} = h_{av\_in} - [h_{av\_out} - h_{vap} \cdot (x_{out} - x_{in})] \tag{22}$$

By combining the total useful change in enthalpy, we can define the efficiency of two phase expander as described below:

$$\eta_{one\_phase} = \frac{W_{generator\_out}}{\dot{m} \cdot [h_{av_{in}} - (h_{av_{out}} - h_{vap} \cdot (x_{out} - x_{in}))]} \quad (23)$$

3.5 Double flash cycle (Back pressure turbine)

This cycle in Figure 5 has some additional equipment with throttling valve in between the separator and flasher to create a flashing of saturated liquid from the separator outlet. The throttling valve function is to make differential pressure or pressure drop at state 2, then the two phase fluids will enter into the flasher in order to separate the steam and water.

The separated steam heads towards the back pressure turbine without condensing process, and the separated water flows into reinjection wells.

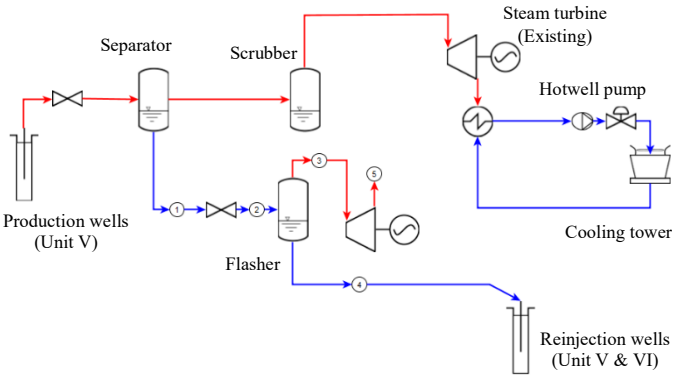

Figure 5: Double flash cycle

The flashing process is isenthalpic, therefore:

$$h_1 = h_2 \quad (24)$$

The steam flow enter into back pressure turbine can be found using:

$$\dot{m}_3 = \dot{m}_2 \cdot x_2 \quad (25)$$

Where the steam fraction of the mixture at state 2, steam flow, isentropic dryness ($s_3 = s_5$), isentropic enthalpy, power and turbine efficiency can be calculated from:

$$x_2 = \frac{h_2 - h_4}{h_3 - h_4} \quad (26)$$

$$\dot{m}_3 = \dot{m}_2 \cdot x_2 \quad (27)$$

$$x_3 = \frac{s_5 - s_{f5}}{s_{g5} - s_{f5}} \quad (28)$$

$$h_5 = h_{f5} + x_3 \cdot (h_{g5} - h_{f5}) \quad (29)$$

$$\dot{W}_{turbine} = \dot{m}_v \cdot (h_{g3} - h_4) \quad (30)$$

$$\dot{W}_{turbine} = \dot{m}_v \cdot \eta_T \cdot (h_{g3} - h_4) \quad (31)$$

3.6 Silica saturation index (SSI)

In order to know if silica scaling could occur or not inside pipe, the silica saturation index value should be found at operation condition. The scaling can occur in the brine if *SSI* more than 1 and if *SSI* is equal to 1 it means the silica is in an equilibrium state. According to the Fournier and Rowe (1977) approach, the solubility of amorphous silica in the water can be obtained:

$$log\ s_o = 4.52 - \left(\frac{731}{T\ (Kelvin)}\right) \quad (32)$$

Then we can calculate the corrected silica solubility in the presence of fluid salinity through equation (Setschenow, Chen and Marshall):

$$log\ D_{(t)} = -1.0569 - 1.573 \cdot 10^{-3} \cdot t \tag{33}$$

$$Salinity\ (m_{Cl}) = \frac{[Cl^-]}{35.5 \cdot 1000} \tag{34}$$

$$s_{eq} = s_o \cdot 10^{-m.D_{(t)}} \tag{35}$$

The last, we can determine of silica saturation index is formulated as follows:

$$SSI = \frac{SiO_{2\ brine}}{s_{eq}} \tag{36}$$

4. PROCESS DESIGN OF HYDROTHERMAL TURBINE AND DOUBLE FLASH CYCLE

4.1 Piping

4.1.1 Pipe size selection

Based on operation/production data and tracer flow test results of unit V, these parameters were used as initial data to design and analysis within this research project:

- Atmospheric pressure = 0.924 bara;
- Separator pressure = 7.676 barg = 8.6 bara;
- Total flow rate of brine = 779.4 ton/hr or 216.5 kg/s (LHD-27, LHD-31, LHD-34).

The new pipeline that will attach in the main line (16" sch. 20) would be chosen size of 6" schedule 40 with inlet diameter 0.15406 m. Using the Bernoulli's principle, it can be defined that the upstream pressure in the new pipe is as a liquid transport to binary turbine.

Then from pressure above, brine velocity was found to be 2.44 m/s, minimum thickness of pipe 6" is 3.43 mm accordance to process piping standard, and other physical properties.

To calculate a flow rate inside pipe 6" schedule 40, using the liquid density from working pressure 8.75 bara, that is 893.14 kg/m^3. The thickness from pipe 6" schedule 40 is greater than minimum thickness needed, 7.11 mm > 3.43 mm, it would prevent the total dissolved solid and acid fluids carried-out from geothermal fluid wells for 30 years, in the planning of design. Moreover, this design will be planned for a flow rate of 40.62 kg/s from the total of mass flow 216.5 kg/s according to the pipe size capacity that has been chosen.

4.1.2 Pressure drop

From the working pressure (upstream side) of 8.75 bara, then the physical properties of liquid can be determined from a steam table to calculate Reynolds number, friction factor, equivalent length and friction head. They relate to obtain pressure drop as summarized in Table 3 with plan of pipe length about 30 meters.

Table 3: Physical properties and pressure drop in pipeline system

No.	Description	Value	Uom
1.	Liquid density (ρ_f)	893.14	kg/m^3
2.	Viscosity (μ_f)	$155.47 \cdot 10^{-6}$	kg/ms
3.	Reynolds number (Re_L)	2 159 456.9	-
4.	Absolute roughness (Є) - commercial steel pipe	$1.5 \cdot 10^{-4}$ $4.57 \cdot 10^{-5}$	ft m
5.	Friction factor (f), Swanee-Jain approach	0.01533	-
6.	Total equivalent length (L_e)	48.59	m
7.	Friction head (H_f)	1.47	m
8.	Pressure drop ($\mathbf{\Delta}P_f$)	12857.99 0.13	Pa bar

So, from result above we can obtained of pressure drop from upstream to downstream along new pipeline is 0.13 bar. In addition, the downstream pressure will be 7.83 barg – 0.13 barg = 7.70 barg or equal to 8.63 bara.

4.1.3 Heat loss along new pipeline

With using a working pressure of 7.83 barg or 8.75 bara, the physical properties of the liquid can be obtained from steam table. Moreover, using an average air temperature of 22.8°C or 295.95K with wind velocity of 0.66 m/s (PT PGE, 2015), the physical properties of air can be obtained from interpolation of atmospheric table values.

This pipe will have an insulation jacket for the purpose of preventing heat loss from internal and external factors that can cause the temperature to fall excessively, as well as for safety purposes. The insulation consists of two layer materials, there are calcium silicate and aluminum sheet with chosen thickness 50 mm and 0.8 mm each (Nugraha, 2018).

Therefore, we can obtain of heat loss along new pipeline:

$$q = \frac{2 \cdot \pi \cdot (174.18 - 22.8) \cdot 30}{\frac{1}{11839.13 \cdot 0.07703} + \frac{\ln 0.0841/0.07703}{67} + \frac{\ln 0.13414/0.08414}{0.072} + \frac{\ln 0.13494/0.13414}{237} + \frac{1}{4.171 \cdot 0.13494}}$$

$$q = 3455.87\ W\ or\ J/s$$

$$\Delta T = \frac{3455.87}{40.62 \cdot 4383.998} = 0.019\ ^{\circ}\mathrm{C}$$

As a result, the end of temperature at downstream side is 174.18°C – 0.019°C = 174.16°C.

4.2 Hydrothermal turbine power (turbo expander)

The hydrothermal turbine will cover the expansion process associated with generating power, so it will have a reduction in saturated liquid pressure from high pressure to low pressure that will vaporize the fluids due to atmospheric condition, caused by a high temperature source. The expansion of saturated liquid or wet vapors can be handled by turbo expander type, and this type can be chosen depending on how much the flow rate due to the influence of the volume ratio relates to dimension itself.

Based on references, as mentioned previously in theoretical background of two-phase expanders, the turbo expander type was selected as the turbine driven by boiling liquid. First, calculating the power output and second, the efficiency of a two-phase expander utilizing the change in internal energy of the operating fluid while taking into account the enthalpy of vaporization. With using equation (16) to (23), then we can find the result as in Table 4 below.

Table 4: The physical properties of turbo expander

No.	Description	Value	Uom	Note
Flashing along pipe 6”				
1.	Upstream pressure (P_0)	7.83	barg	
		8.75	bara	
2.	Enthalpy of sat. liquid (h_{f0})	737.56	kJ/kg	
Flashing inside turbo expander				
3.	Downstream pressure (P_1) – inlet	7.70	barg	
		8.63	bara	
4.	Enthalpy of sat. liquid (h_{f1})	734.82	kJ/kg	
5.	Enthalpy of sat. vapor (h_{g1})	2771.35	kJ/kg	
6.	Entropy of sat. vapor (s_1 or s_{g1})	6.64	kJ/(kg·K)	$s_1 = s_{g1} = s_2$ (Isentropic process)
7.	Latent heat of evaporation (h_{fg1} or h_{vap})	2036.53	kJ/kg	
8.	Atmospheric pressure (P_{atm})	0.924	bara	
9.	Outlet pressure (P_2) – outlet	5.924	bara	as Kimmel (2010) mention
10.	Enthalpy of sat. liquid (h_{f2})	668.34	kJ/kg	
11.	Enthalpy of sat. vapor (h_{g2})	2755.58	kJ/kg	
12.	Latent heat of evaporation (h_{fg2} or h_{vap})	2087.24	kJ/kg	
13.	Entropy of sat. liquid (s_{f2})	1.93	kJ/(kg·K)	
14.	Entropy of sat. vapor (s_{g2})	6.76	kJ/(kg·K)	
15.	Proportion of flash steam (x_1) – inlet	0.13	%	Inside pipe and expander
16.	Dryness (x_2) – outlet	97.36	%	Outlet pressure, isentropic ($S_1 = S_2$)

This process emerges the flash steam around 0.13% when the brine has flowed into pipe 6", from pipe 16" (main line). This may occur due to a pressure drop inside pipe 6" from the upstream to downstream side. The steam also flashes during exit from turbo expander, at about 97.36% to the atmosphere, but it has the optimum set of back pressure 5 bar to minimize vapor during expansion process in the turbo expander.

From Figure 6, the low outlet pressure can obtain a high power, but will have more steam in the expander.

The other hand, a proportion of steam appears from boiling liquid, the brine starts to boil when it gets into pipe 6", the temperature has increase inside the pipe and temperature inside pipe 6" is higher than saturation temperature inside pipe 16" because of an increase in pressure. The sequences to obtain power output is shown in Table 5.

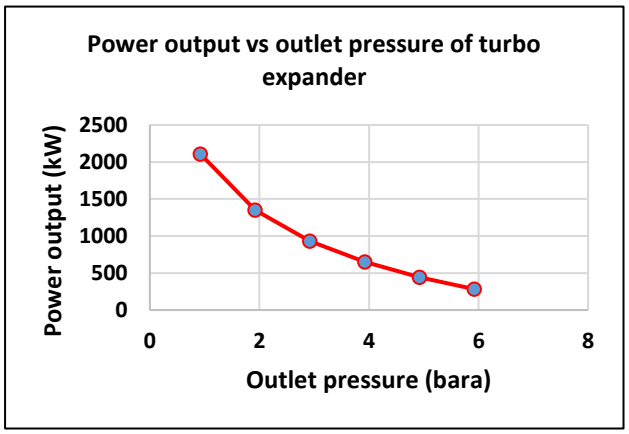

Figure 6: Turbo expander optimization

Table 5: The power output of turbo expander

No.	Description	Value	Uom	Note
1.	Total flow rate (m_{tot})	40.62	kg/s	During entrance to the turbo expander
2.	Vapor flow rate (m_v)	0.05	kg/s	
3.	Liquid flow rate (m_l)	40.57	kg/s	
4.	Mixture enthalpy (h_m or h_{av}) – inlet	737.56	kJ/kg	
5.	Mixture enthalpy (h_m or h_{av}) – outlet	2700.5	kJ/kg	
6.	The energy use in vaporization process	1980.05	kJ/kg	
7.	The useful change in enthalpy (**Δ**h)	17.1	kJ/kg	
	or equal to:			
8.	Work output of turbo expander (W_{max})	17.1	kJ/kg	
9.	Power output (W generator out)	694.74	kW or kJ/s	In an ideal power output (100% of efficiency)
		694738.83	W or J/s	
10.	Efficiency (η)	40.62	%	
11.	Power output with the eff. (W final)	282.23	kW	The actual power output

The power output from the turbo expander was 282.23 kW with an efficiency of 40.62%. The power has been obtained just from the liquid enthalpy, not including the vapor phase inside the expander. So, the efficiency couldn't reach too high, as expected.

4.3 Scenario and power using double flash cycle (back pressure)

In this case, double flash cycle, it would use the entire brine flow rate from production separator unit V Lahendong, around 216.5 kg/s, to generate the back pressure turbine. The pressure drop between state 1 and 2 would be assumed have range from 1.9, 3.8, and 5.7 bara relates to the optimization results and *SSI*. Furthermore, the other assumptions are:

- No pressure drop in the steam pipe and inside flasher separator;
- No heat loss in the pipeline system;
- Flasher separator efficiency is neglected and isentropic turbine efficiency is 85%.

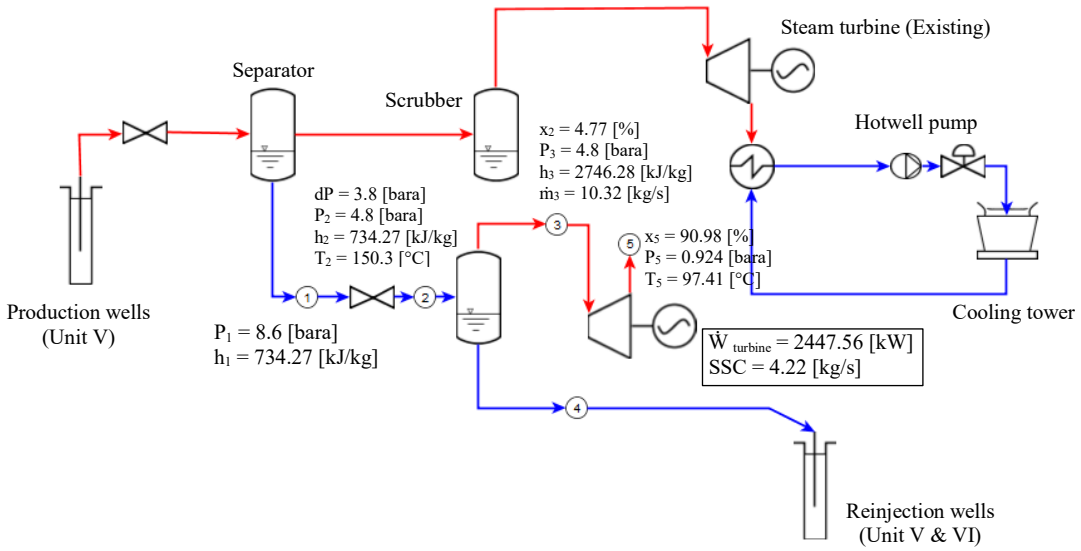

Figure 7: Double flash cycle output

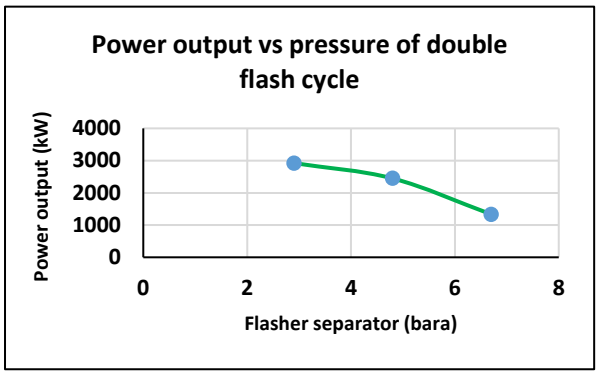

Figure 8: Power output vs flasher pressure

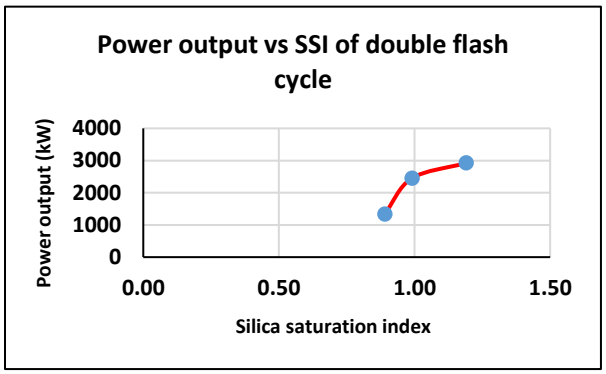

Figure 9: Power output vs SSI

Figure 7 explains that the optimum power output of the double flash cycle is 2447.56 kW with a flasher separator pressure of 4.8 bara. The output is chosen due to consideration of the saturation temperature and working pressure on the flasher separator. It requires that the pressure is not too low with the hot brine such that there is an adequate pressure to flow it into the reinjection wells. Moreover, the *SSI* value from this cycle is 0.99, and it will increase when the working pressure of the flasher separator has a low setting as described in Figure 8 and Figure 9.

The P-h diagram, as shown in Figure 10, explains that the higher pressure of the flasher separator will acquire a low dryness in the mixture area, and the opposite with the lower pressure setting. However, the enthalpy does not change when the pressure of main separator is equal to upstream side of double flash cycle.

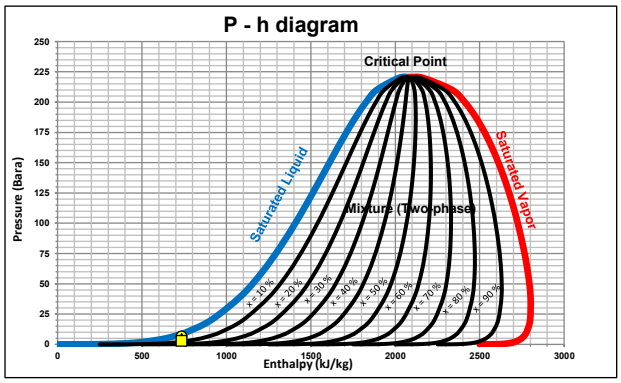

Figure 10: P - h diagram

The enthalpy of the production separator is equal to the flasher separator and since the production separator pressure has no change in the short or long term, the flasher enthalpy would be equal. However, the change in pressure on the flasher separator will be followed by the changes in the steam fraction and steam flow, the lower pressure will be obtained from the high steam fraction.

4.4 Silica saturation index (SSI)

The laboratory tests result from the separator of unit V on 25 June 2018 (PT PGE, 2018), some of the data is presented:

- pH = 8.6;
- S_iO_2 & Cl^- = 620 mg/l;
- Cl^- = 705 mg/l.

In this pipeline the system had heat loss of about 0.019°C and gave the temperature at the end of pipe of 174.16°C. Accordance to given equations, we can describe the silica saturation index through actual condition parameters as described in Table 6 below.

Table 6: Silica saturation index in different temperature

No.	Description	Value	Uom
Brine temp. = 174.16°C at downstream side			
1.	Log s_o - Fournier and Rowe (1977)	2.8858	-
	Solubility of amorphous silica in water (s_o)	768.776	mg/l
2.	D_t - Chen and Marshall equation	0.04668	-
3.	Salinity (m_{Cl})	0.0199	mol/l
4.	Corrected of silica solubility (s_{eq}) - Setschenow eq.	767.14	mg/l
5.	Silica saturation index (SSI)	0.8082	-
Silica scaling start to formed at temperature = 150°C and below it			
1.	Log s_o - Fournier and Rowe (1977)	2.7925	-
	Solubility of amorphous silica in water (s_o)	620.126	mg/l
2.	D_t - Chen and Marshall equation	0.05095	-
3.	Salinity (m_{Cl})	0.0199	mol/l
4.	Corrected of silica solubility (s_{eq}) - Setschenow eq.	618.68	mg/l
5.	Silica saturation index (SSI)	1.0021	-

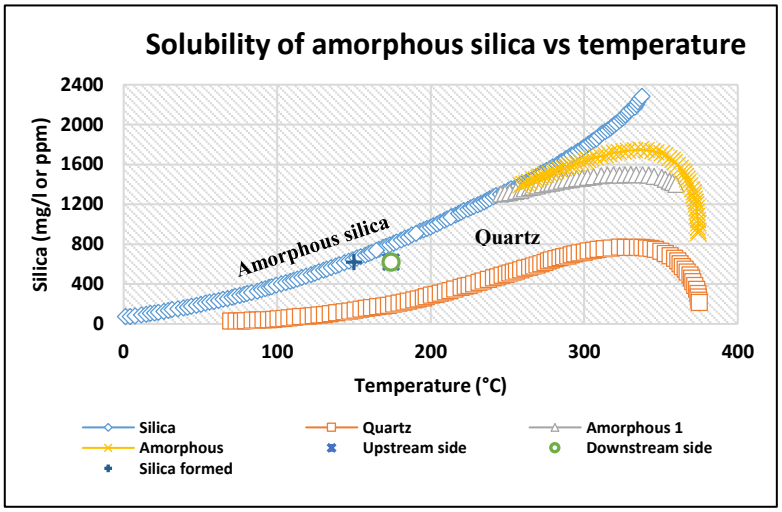

Figure 11: Amorphous silica vs temperature

The *SSI* in this project would occur if it reaches a temperature of about 150°C or less as in Figure 11, it will be inside the amorphous silica zone, so it should be considered to produce power from each turbine.

5. CONCLUSIONS

The use of working pressure and hot brine from production separator in this research project have the opportunity in develop a secondary power generation. The project activities can be conducted while the power plant unit V and production wells are shut down or not in production for around 2 days due to having some modification/construction to make a new branch from the production separator main line (brine pipe). The chosen pipe size is 6" schedule 40 and it was considered to not disturb the operation parameters needed for main production.

The process design of hydrothermal turbine is using two phase expanders, the turbo expander related with the common technology and has been proved in LNG plants to generate a power from boiling liquid. The turbo expander has methods to generating power from two phase fluids, it removes the vapor energy or vaporization process from the system for the real work of turbine. Furthemore, the turbo expander has a set of back pressure in the outlet of about 5 bar to prevent excess steam that will remain inside the turbine.

The last part in this research project is using a back pressure turbine as a double flash cycle system and is able to generate power at around 2447.56 kW. The optimization was chosen due to consideration of SSI value and working pressure in the flasher separator of 4.8 bara in order to flow the hot brine into reinjection wells.

However, double flash cycle either with condensing or non-condensing types have a great consideration in the next green field projects at PT Pertamina Geothermal Energy. The secondary power from this cycle would contribute to adding more power and should be designed at initial project phase, so it will not interfere with operations and production activities when it will be developed (Nugraha, 2018).

REFERENCES

Finley, C. D., 2006: Definition of hydraulic efficiency of two-phase expanders driven by boiling liquid. Ebara International Corporation, Sparks NV. *AIChE Spring Meeting*, *6th Topical Conference on Natural Gas Utilization*, *April 23-27*, Orlando-Florida, 6 pp.

Fournier, R. O., and Rowe, J. J., 1977: The solubility of amorphous silica in water at high temperatures and high pressures. *Am. Min.*, 62, 1052-1056.

Kimmel, H. E., Cathery, S, 2010: Thermo fluid dynamics and design of liquid-vapor two-phase LNG expanders. *GPA paper*, 9 pp.

Nugraha, A. S., 2018: Process design of micro hydro, expander, binary orc and double flash cycle using separator pressure of unit V in Lahendong geothermal field, Indonesia. UNU-GTP, Iceland, unpublished reports, 62 pp.

PT PGE, 2015: *Lahendong unit 5&6 geothermal power project of BEDD, As built document*. PT Pertamina Geothermal Energy, Lahendong area, Indonesia, unpublished report, 25 pp.

PT PGE, 2017: *Tracer flow test report of LHD cluster 27*. PT Pertamina Geothermal Energy, Lahendong area, Indonesia, unpublished report.

PT PGE, 2018: *Geochemist laboratory analysis of Lahendong geothermal field*. PT Pertamina Geothermal Energy, Lahendong area, Indonesia, unpublished report.

PT PGE, 2019: *Working areas*. PT Pertamina Geothermal Energy, website: www.pge.pertamina.com.